

Multivalent Antiviral XTEN–Peptide Conjugates with Long in Vivo Half-Life and Enhanced Solubility

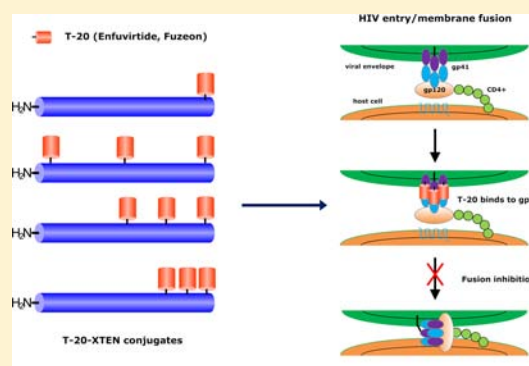
Sheng Ding,[†] Michael Song,[†] Bee-Cheng Sim,[†] Chen Gu,[†] Vladimir N. Podust,[†] Chia-Wei Wang,[†] Bryant McLaughlin,[†] Trishul P Shah,[‡] Rodney Lax,[‡] Rainer Gast,[‡] Rahul Sharan,[‡] Arthur Vasek,[‡] M. Amanda Hartman,[†] Colin Deniston,[†] Prathna Srinivas,[†] and Volker Schellenberger^{*,†}

[†]Amunix Operating Inc., 500 Ellis Street, Mountain View, California 94043 United States

[‡]PolyPeptide Laboratories Inc., 365 Maple Avenue, Torrance, California 90503 United States

S Supporting Information

ABSTRACT: XTENs are unstructured, nonrepetitive protein polymers designed to prolong the in vivo half-life of pharmaceuticals by introducing a bulking effect similar to that of poly(ethylene glycol). While XTEN can be expressed as a recombinant fusion protein with bioactive proteins and peptides, therapeutic molecules of interest can also be chemically conjugated to XTEN. Such an approach permits precise control over the positioning, spacing, and valency of bioactive moieties along the length of XTEN. We have demonstrated the attachment of T-20, an anti-retroviral peptide indicated for the treatment of HIV-1 patients with multidrug resistance, to XTEN. By reacting maleimide-functionalized T-20 with cysteine-containing XTENs and varying the number and positioning of cysteines in the XTENs, a library of different peptide–polymer combinations were produced. The T-20-XTEN conjugates were tested using an in vitro antiviral assay and were found to be effective in inhibiting HIV-1 entry and preventing cell death, with the copy number and spacing of the T-20 peptides influencing antiviral activity. The peptide–XTEN conjugates were also discovered to have enhanced solubilities in comparison with the native T-20 peptide. The pharmacokinetic profile of the most active T-20-XTEN conjugate was measured in rats, and it was found to exhibit an elimination half-life of 55.7 ± 17.7 h, almost 20 times longer than the reported half-life for T-20 dosed in rats. As the conjugation of T-20 to XTEN greatly improved the in vivo half-life and solubility of the peptide, the XTEN platform has been demonstrated to be a versatile tool for improving the properties of drugs and enabling the development of a class of next-generation therapeutics.



INTRODUCTION

Protein and peptide therapeutics play a pivotal role in modern medicine for the treatment and prevention of serious diseases. However, many protein and peptide drugs suffer from short in vivo half-lives which limit their therapeutic applications. Much recent effort has been focused on the development of “biobetter” molecules with extended plasma half-lives to reduce their administration frequencies and to extend their therapeutic windows.¹ Notably, the conjugation of biotherapeutics to poly(ethylene glycol) (PEG) remains a widely used technique for prolonging the in vivo half-lives of these drugs, and numerous PEGylated drugs have been clinically approved.^{2–4}

XTEN protein polymers are recombinant PEG mimetics designed to improve the performance of protein and peptide pharmaceuticals while avoiding many of the disadvantages of PEG.⁵ XTENs are highly hydrophilic, unstructured polypeptides composed entirely of alanine, glutamate, glycine, proline, serine, and threonine residues. When recombinantly fused with XTEN, the so-called XTENylated bioactive proteins and peptides typically exhibit 60- to 130-fold increases, depending

on the payload, in their in vivo half-lives over their native counterparts.^{5–9}

By increasing the hydrodynamic radius and providing steric shielding for its payloads, XTEN functions in a manner similar to PEG, but with several key differences. While large molecular weight PEGs are polydisperse mixtures whose coupling to payloads often results in heterogeneous products, XTEN proteins have precise, genetically defined chemical compositions, eliminating product heterogeneity and greatly promoting their ease of manufacture. In addition, because PEGs are chemical polymers that cannot be metabolized or degraded after administration, they have been known to cause unwanted side effects such as cellular vacuolation upon continuous treatment.¹⁰ In contrast, XTEN is rapidly degraded upon its internalization into cells, and its biodegradable nature typically results in its decreased accumulation in tissues and reduced

Received: May 15, 2014

Revised: June 13, 2014

Published: June 16, 2014

potential for toxicity. Finally, as XTEN has been engineered to be resistant to plasma proteases, it can remain intact for a significant period of time while in circulation.

With these properties, the XTEN platform shows great potential to be a superior tool for half-life extension compared with PEGylation. Two XTEN-based products, human growth hormone-XTEN (VRS-317) and exenatide-XTEN (VRS-859), are currently being evaluated in clinical trials. VRS-317 has been shown to have superior pharmacokinetic and pharmacodynamic properties in comparison with other recombinant human growth hormone products, with the potential for once-monthly dosing,^{7,9} whereas VRS-859 has recently been reported to be effective for patients suffering from type 2 diabetes without the occurrence of significant adverse events (unpublished data).

An additional feature of XTEN is its low theoretical pI of 2.6 which results in it having a net negative charge at neutral pH, enabling it to be purified by anion exchange chromatography. XTENylated proteins and peptides are typically characterized by enhanced solubilities and reduced propensities for aggregation. For example, the molar solubility of a glucagon-XTEN fusion protein was increased 60-fold over that of the native peptide, enabling liquid formulation for the product.⁸

To broaden the applicability of the XTEN platform, we have also recently explored chemical conjugation techniques to attach bioactive payloads to XTEN,¹¹ permitting the application of our XTEN technology to a broader range of drug classes including nonpeptide small molecules that cannot be recombinantly fused to XTEN. Chemical conjugation techniques also enable the incorporation of multiple copies of a drug at defined positions along the XTEN protein, circumventing the constraint of end-to-end fusion which is required by the recombinant format.

In this study, we demonstrate the feasibility and versatility of multivalent drug display through XTENylation using the anti-retroviral peptide T-20 as a model therapeutic payload. T-20, also known as Fuzeon or enfuvirtide, is a linear 36 amino acid synthetic peptide derived from the C-heptad repeat region of human immunodeficiency virus type 1 (HIV-1) envelope glycoprotein (Env) transmembrane subunit gp41. T-20 works as a potent inhibitor of viral infections by preventing HIV-1 from fusing with and entering host cells.¹² By interacting with the N-heptad repeat region of viral gp41 and blocking gp41 six-helix bundle core formation, it inhibits a critical step in virus–cell fusion and prevents the virus from entering into uninfected cells.¹³

As a peptide fusion inhibitor administered by subcutaneous injection, T-20 was the first of a novel class of anti-retroviral drugs and was approved by the US FDA in 2003. It is indicated, in combination with other anti-retroviral pharmaceuticals, for the treatment of HIV-1 patients with multidrug resistance. Despite its therapeutic efficacy, its market acceptance has been limited due to several shortcomings.¹⁴ First, T-20 has a short plasma half-life which necessitates twice-daily injections of the drug. Second, T-20 has extremely poor solubility in water and is supplied as a lyophilized powder which requires an inconvenient 45 to 60 min resolubilization step prior to administration. Injection site reactions which are often painful occur in up to 98% of patients.¹⁵ In this study, we report the conjugation of one or three copies of T-20 to XTEN in different configurations, demonstrating the versatility of the platform and addressing many of the shortcomings of T-20 by imparting improvements through the half-life and solubility of the T-20-XTEN conjugates.

RESULTS

Expression and Purification of XTEN Protein Precursors. Maleimide–thiol chemistry is a commonly used technique in protein conjugation and was selected for use in this work. To evaluate the effects of copy number and spacing on the antiviral activity of T-20-XTEN conjugates, four versions of cysteine-containing XTENs (XTEN-1, 2, 3, 4) were designed for conjugation with maleimide-functionalized T-20 (Figure 1).

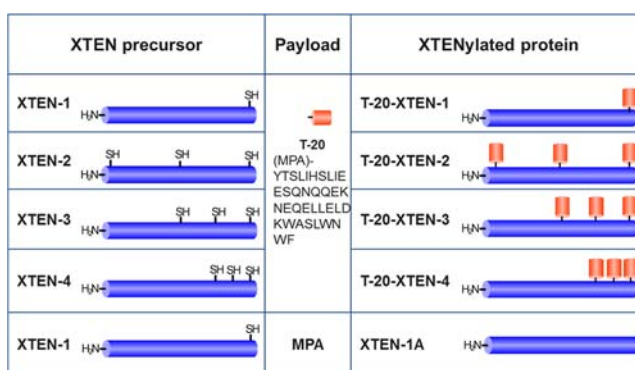


Figure 1. Schematic representations of the constructs used in the studies. There are four XTEN precursor molecules, and by conjugating them to the payload T-20 or MPA, five different XTENylated proteins were synthesized.

Each of the XTEN precursors was composed of 432 amino acids, with XTEN-1 containing only one cysteine and XTEN-2, 3, 4 each containing three cysteines with different inter-cysteine spacings.

The proteins were expressed and purified using a modified version of a protocol previously described for 1×Amino-XTEN864.¹¹ The constructs were designed with an N-terminal helper tag engineered to enhance XTEN expression in *E. coli* and a C-terminal histidine tag designed to ensure the integrity of the C-terminus following the initial IMAC purification step. The tags were fully cleavable by trypsin digestion as they were separated from the XTEN sequence by arginine residues.

The proteins were first passed through an IMAC capture column following clarification of the crude lysate. The eluates were found to be mostly pure based on SDS-PAGE analysis with Coomassie staining, and the pools were digested with trypsin. After confirming tag removal by MALDI-TOF MS and inactivating any residual trypsin, the mixtures were further purified using anion exchange chromatography (AEX), concentrated, and then formulated into storage buffer. The formulated proteins were characterized by SDS-PAGE with silver staining and C4 RPC, with the products determined to be more than 90% pure. The proteins were additionally analyzed by ESI-MS and their concentrations determined by amino acid analysis. Size exclusion chromatography (SEC) indicated that more than 90% of the proteins were monomeric and they exhibited a large hydrodynamic radius exceeding that of the 160 kDa standard, in accordance with previous observations made for XTEN proteins.⁵ Characterization results are not shown as they are discussed in a previous publication.¹¹

Production of T-20-XTEN Conjugates. The thiol-containing XTEN precursors were reacted with MPA-T-20 at ambient temperature to form the 1× and 3×T-20-XTEN conjugates. Prior to conjugation, XTEN-1 is manifested as two peaks in C4 RPC, representing the XTEN-1 monomer and a

suspected disulfide-bonded dimer at 20.2 and 21.2 min, respectively (Supporting Information, Figure S1). The hydrophobic T-20 peptide had a significantly greater retention time at 43 min. After incubating the reaction mixture for 2 h at 25 °C, a new peak was observed at 37.2 min, which was confirmed by ESI-MS to be the T-20-XTEN-1 conjugate (Figure 2). The

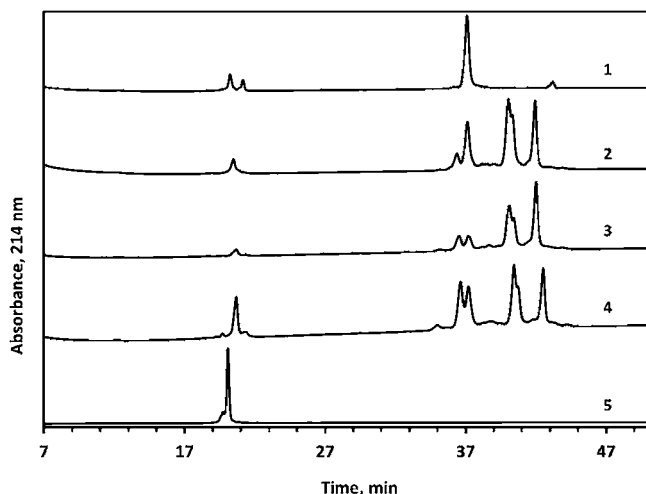


Figure 2. HPLC monitoring of chemical conjugation reactions. 1: XTEN-1 and T-20 reaction mixture at 2 h time point; 2: XTEN-2 and T-20 reaction mixture at 8 h time point; 3: XTEN-3 and T-20 reaction mixture at 8 h time point; 4: XTEN-4 and T-20 reaction mixture at 8 h time point; 5: XTEN-1 and MPA reaction mixture at 2 h time point.

conversion of the XTEN-1 precursor into the conjugate was approximately 79%, and the product peak was distinctly separated from both the XTEN precursor and the T-20 peptide in C4 RPC. The large scale synthesis was performed under similar conditions.

Pilot-scale syntheses were also performed for the XTEN precursors containing 3 cysteine residues (XTEN-2, 3, 4). Increasing the molar excess of MPA-T-20 to the thiol-containing XTEN precursors resulted in increased conversions to the 3×T-20-XTEN conjugates (data not shown), but it was challenging to separate unreacted MPA-T-20 from the 3×T-20-XTEN conjugates on preparative C4 RPC because they eluted with similar retention times. AEX chromatography was explored as an alternative strategy for separating the 3×T-20-XTEN conjugates from unreacted peptide, but it did not display any obvious advantages over preparative C4 RPC in terms of resolution. To ensure the purity of the final T-20-XTEN conjugates, the large scale syntheses were performed in stoichiometric amounts at a molar ratio of 3:1 (MPA-T-20:XTEN).

Under these conditions, MPA-T-20 was found to be mostly consumed after 4 h at 25 °C as no peaks were observed with a similar retention time as the peptide control, whereas multiple new peaks appeared with retention times ranging from 35 to 43 min (Figure 2). As more copies of T-20 peptide were introduced to the XTEN molecules, the hydrophobicity of the T-20-XTEN conjugates increased, with a corresponding increase in their retention times. Based on peak analysis by ESI-MS, the proteins eluting from 35.0 to 38.5 min represented conjugates containing a single copy of T-20, those from 39.0 to 41.0 min represented conjugates containing two copies of T-20, and those from 41.5 to 42.5 min represented conjugates containing the full three copies of T-20. Because T-20 could be

conjugated to any of the three cysteines at different positions on the XTEN precursors, the incompletely reacted 1× and 2×T-20-XTEN conjugates were found to manifest as isomers appearing as multiple peaks on analytical C4 RPC. When the 3×Thiol-XTENs were functionalized with all three copies of T-20, only one isomeric form was possible, resulting in a single peak for the 3×T-20-XTEN conjugate.

Biophysical Characterization of XTENylated Peptides.

The purified XTENylated peptides were analyzed using multiple techniques to confirm their quality. Each of the T-20-XTEN conjugates was found to migrate as a single band by SDS-PAGE analysis (Figure 3A). Their apparent molecular

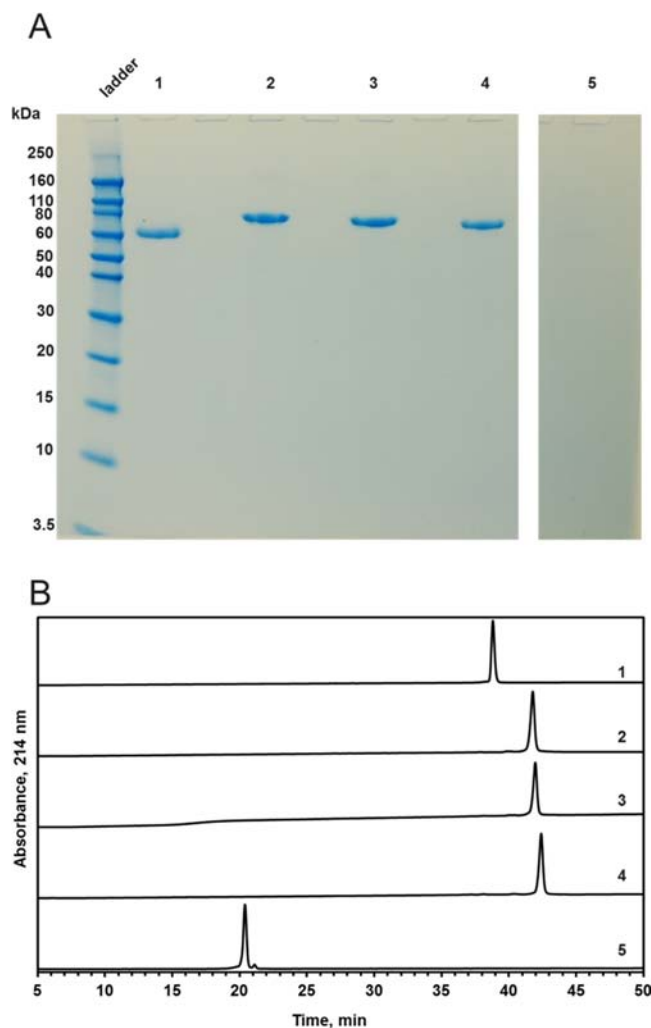


Figure 3. Analytical characterization of the purified XTEN conjugates. A. SDS-PAGE gel with Coomassie staining: Lane 1, T-20-XTEN-1; Lane 2, T-20-XTEN-2; Lane 3, T-20-XTEN-3; Lane 4, T-20-XTEN-4; Lane 5, XTEN-1A. B. HPLC profiles: 1, T-20-XTEN-1; 2, T-20-XTEN-2; 3, T-20-XTEN-3; 4, T-20-XTEN-4; 5, XTEN-1A.

weights fell between 60 and 80 kDa, which was greater than the calculated weights of 44.0 kDa for the 1×T-20 conjugate and 53.2 kDa for the 3×T-20 conjugates. This confirms a phenomenon which is commonly observed for XTEN derivatives.⁵ The proteins were found to elute as single, sharp peaks on analytical C4 RPC (Figure 3B). It was not possible to visualize the negative control (XTEN-1A) via Coomassie staining, but it was confirmed to have greater than 90% purity by C4 RPC. The molecular weights of the five compounds were

also verified by ESI-MS, with the observed masses found to be in agreement with the calculated masses for all of the molecules (data not shown).

Because the proteins were formulated at concentrations exceeding 15 mg/mL, aggregation was a concern. The XTENylated peptides were characterized by dynamic light scattering (DLS) at their formulated concentrations (Table 1).

Table 1. Summary of DLS Results for the XTEN Conjugates

protein	stock concentration (mg/mL)	effective radius at stock conc. (nm)	aggregation by intensity, %	aggregation by mass, %
T-20-XTEN-1	13.23	2.6	0	0
T-20-XTEN-2	18.46	2.8	25.4	0
T-20-XTEN-3	9.48	3.5	24.1	0
T-20-XTEN-4	25.03	2.5	16.5	0
XTEN-1A	18.46	2.0	0	0
BSA (not heat treated)	2	2.6	0	0
BSA (heat treated)	2	3.1	92.2	28

The effective radii for the T-20-XTEN conjugates were measured to be between 2.5 and 3.5 nm, whereas XTEN-1A was shown to exhibit an effective radius of 2.0 nm. While some aggregation by intensity was observed for the 3×T-20-XTEN conjugates, aggregation by mass was used as a more quantitative measure as aggregated molecules are known to produce disproportionately strong signals when measured by intensity with DLS. Based on aggregation by mass, all the T-20-XTEN conjugates displayed negligible amounts of aggregation in solution, indicating that they formed negligible higher-order interactions under the selected formulation conditions. The heat-treated BSA which was used as a positive control formed aggregates when assayed under the same conditions.

Antiviral Activity of the T-20-XTEN Conjugates. We used an in vitro cell-based MAGI assay to characterize the antiviral activity of the XTENylated peptides. Peptide-XTEN conjugates were incubated with MAGI CCR5 cells prior to introduction of HIV-1_{Ba-L} to the mixtures. While all of the compounds exhibited negligible toxicities with TC₅₀ values exceeding 10 000 nM, all of the T-20-XTEN proteins were discovered to have dose-dependent antiviral activity (Figure 4). The T-20 peptide alone had an IC₅₀ of 0.38 nM, in agreement with published values (Table 2), while the negative control (XTEN-1A) did not exhibit any discernible antiviral effects. In general, the T-20-XTEN conjugates exhibited more than 30-fold reductions in their antiviral activities compared with the native peptide. However, trends in activity were observed among the individual T-20-XTEN conjugates. T-20-XTEN-1, which contained a single copy of T-20, had an IC₅₀ of 160.7 nM, whereas T-20-XTEN conjugates containing 3 copies of T-20 (T-20-XTEN-2, 3, 4) exhibited substantially stronger antiviral activities, indicating that multivalent display of the peptide did improve the activity of the conjugates. Among the 3×T-20-XTEN conjugates, the construct with the most closely spaced peptides, T-20-XTEN-4 (51 amino acids apart), exhibited the strongest antiviral activity with an IC₅₀ of 12.9 nM, followed by the less closely spaced T-20-XTEN-3 (102

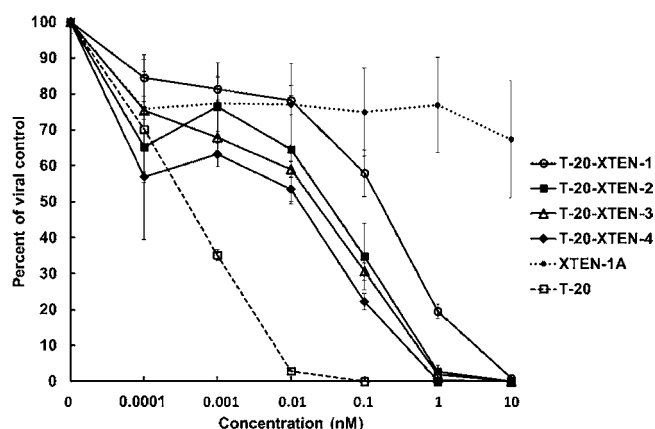


Figure 4. In vitro antiviral activity of XTENylated peptides. A MAGI antiviral assay was performed to assess the antiviral activity of the XTENylated peptides. The β -galactosidase enzyme activities of the MAGI cells were quantified as a measurement of virus amount and presented as a percentage of the blank concentration, defined to be 100%.

Table 2. Summary of the Antiviral Activity of the Compounds Tested by MAGI Assay^a

Sample	IC ₅₀ (nM)	TC ₅₀ (nM)
T-20	0.38	>10,000
XTEN-1A	>10,000	>10,000
T-20-XTEN-1	160.7	>10,000
T-20-XTEN-2	30.7	>10,000
T-20-XTEN-3	20.7	>10,000
T-20-XTEN-4	12.9	>10,000

^aIC₅₀ and TC₅₀ value for the compounds were calculated from the MAGI antiviral assay and the MTS cytotoxicity assay, respectively.

amino acids apart) with an IC₅₀ of 20.7 nM, and finally, the least closely spaced T-20-XTEN-2 (204 amino acids apart) with an IC₅₀ of 30.7 nM. These results demonstrate that T-20 retains its antiviral activity even following conjugation to XTEN, and that the activity of the peptide-XTEN conjugates can be tuned by varying the copy number as well as the positioning of the peptides.

Prolonged in Vivo Half-Life of the Conjugates. The pharmacokinetics of the most active XTEN-conjugate, T-20-XTEN-4, was assayed in rats. As shown in the time-course profile in Figure 5, the pharmacokinetic profile of T-20-XTEN-4 was characterized by an absorption phase which led to a maximum plasma concentration C_{max} of 11.1 mg/mL at 24 h, followed by a linear elimination phase. The calculated elimination half-life of T-20-XTEN-4 was 55.7 ± 17.7 h, almost 20 times longer than the 2.8 h half-life reported for T-20 dosed in rats.¹⁶

DISCUSSION

XTEN was originally designed as a recombinant delivery system for fused peptides or proteins to enhance their plasma half-lives and solubility.^{5,6,8} As a chemically defined, monodisperse protein polymer, XTEN avoids several key limitations of PEG including product heterogeneity, nonbiodegradability,

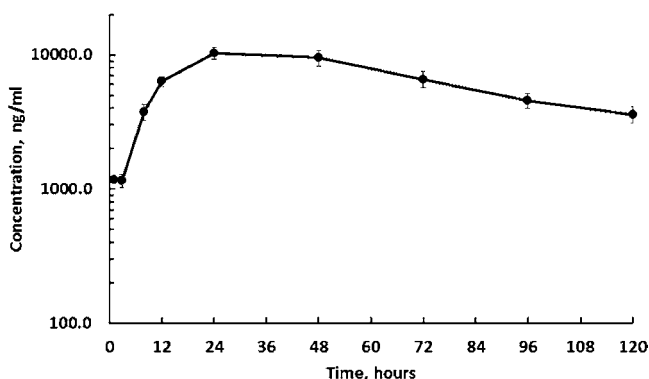


Figure 5. Pharmacokinetics of T-20-XTEN-4 in rats. The compound was administered by subcutaneous injection to three rats at 1.8 mg/mL. Blood samples were collected at different time points, processed to plasma, and stored at -80°C until analysis. Plasma samples were analyzed using an anti-XTEN/anti-XTEN sandwich ELISA. The half-life was determined to be 55.7 ± 17.7 h, and C_{max} was calculated to be $11\,121 \pm 1838$ ng/mL.

and potential toxicity.^{10,17} In contrast to other recombinant half-life extension technologies, e.g., Fc and albumin fusion, XTENylation allows for fine-tuning the in vivo half-life of the therapeutic as the length and composition of the XTEN protein is fully adjustable.

With the expansion of the XTEN technology into chemical conjugation, the versatility in XTEN's applicability to drug classes has been increased, enabling, for example, the covalent attachments of D-, non-natural, and modified amino acid-containing peptides or proteins as well as organic molecules which were previously unattainable with genetic fusion. In addition, chemical conjugation permits cross-linking of multiple copies of monospecific molecules to XTEN polymers in any chosen orientation, as well as of different drug classes to the same XTEN polypeptide via orthogonal chemistries. These conjugates are achievable with precise positioning of chemically reactive amino acids, resulting in products of defined chemical structure and composition.

The goal of this study was to employ the versatile XTEN polymer as a novel platform for multivalent drug display. We chose T-20 as a model peptide for use in this study, with the goal to improve its therapeutic properties through XTENylation. Although T-20 is a clinically approved anti-HIV drug, it is notoriously difficult to work with due to its extremely poor solubility and its short in vivo half-life. Data from the literature indicated that incorporation of multiple copies of T-20 or its derivatives had the potential to increase the antiviral activity of its associated conjugates.^{18,19} With the XTEN platform, we were able to take advantage of increased multivalency and avidity by introducing multiple copies of T-20 to XTEN. This benefit was confirmed by the results of the MAGI antiviral assay, with the T-20-XTEN conjugates containing three copies of T-20 exhibiting stronger activities than the conjugate containing only a single copy of T-20 (overall a 5- to 12-fold increase in potency). In addition to copy number, spacing of the T-20 peptides was also essential in determining the antiviral activity of the conjugates. Previously, Francis et al. tested peptide spacing in a series of branched PIE12-trimers using PEG linkers of various lengths, and they found that the PEG₄ linker resulted in the most improved antiviral potency in comparison with PEG₂, PEG₃, and PEG₅ linkers.²⁰ We also explored the effect of T-20 spacing on antiviral activity, with the

rationale that proper spacing and positioning of the T-20 peptides could facilitate bridging between neighboring hydrophobic pockets in the N-trimer coiled coil region and improve the antiviral activity of the conjugates through promoting avidity. However, if the T-20 peptides were too closely spaced, steric hindrance could conceivably inhibit their activity by preventing T-20 from binding to the deep hydrophobic pockets. Among the three different spacings we tested, the most densely spaced 3×T-20-XTEN conjugate, T-20-XTEN-4, displayed the strongest antiviral activity. Using XTEN as a platform for chemical conjugation, it was possible to produce and characterize a library of constructs in an efficient manner to explore the optimal copy number and spacing for the T-20-XTEN conjugates.

While we screened several conjugates to determine the optimal configuration for antiviral activity, the most promising conjugate still exhibited a 30-fold decrease in activity in the MAGI assay in comparison with the native T-20 peptide. Similar in vitro activity reductions have been observed for XTENylated proteins produced recombinantly in previous studies.^{6,7} For example, 12- and 50-fold in vitro potency reductions were observed, respectively, for human growth hormone and glucagon-like peptide 2 which had been fused with XTEN. This decrease in in vitro activity is most likely caused by steric hindrance involving XTEN, a phenomenon which is also observed with PEGylated ligands. On the other hand, in the same studies involving XTENylated human growth hormone and glucagon-like peptide 2, we have seen increased in vivo efficacies for the XTENylated products despite observed reductions in in vitro activity.^{6,7} Therefore, we suggest that in many cases, the reduction in in vitro activities of the XTENylated ligands may be more than compensated for by the longer efficacious exposures due to the extensions in biological half-life, and we can also predict an increase in in vivo potency for the T-20-XTEN conjugates due to their prolonged exposure in the body. In addition, new constructs can be designed to further improve the activity of the conjugates in future studies. For instance, additional copies of T-20, more densely spaced distributions of T-20, and different XTEN lengths can be easily introduced and characterized using the XTEN platform. Recent developments of peptides related to T-20 have resulted in new drugs with improved potencies over T-20, and these can also be incorporated into XTEN. For example, the D-peptides developed by Welch et al. were reported to exhibit increased antiviral potencies of up to 3 orders of magnitude,¹⁹ and they are compatible for conjugation with XTEN.

The succinimide thioethers formed by the maleimide–thiol reaction used in this study are known to undergo exchange reactions in the presence of other thiol-containing compounds, resulting in the loss of the T-20 payload. To characterize the stability of the succinimide thioethers, we previously evaluated the in vitro plasma stability of the thioether bond in XTENylated proteins produced using the same chemistry, and the half-life of the bond was determined to be greater than 10 days.¹¹

Another key objective of the study was to evaluate XTEN's utility for improving the half-life of the T-20 peptide. The most densely spaced conjugate T-20-XTEN-4 not only exhibited the strongest antiviral activity, it also possessed a prolonged in vivo half-life of 55.7 ± 17.7 h in rats, with the potential to translate to weekly or monthly dosing regimens in humans. The observed half-life is 20-fold longer than the 2.8 h half-life of

precursors were cloned into a pET-30 based vector (Novagen) as described in a previous paper.⁵

XTEN Expression. All of the thiol-containing XTEN precursors (XTEN-1, 2, 3, 4) were expressed in the BL21 *E. coli* strain (New England Biolabs, #C2530H) using 5 L B. Braun Biostat B glass-jacketed fermentation vessels. 125 mL starter cultures were used to inoculate 1.7 L batches of fermentation media containing 50 mM $(\text{NH}_4)_2\text{SO}_4$, 20 mM K_2HPO_4 , 15 mM KH_2PO_4 , 4.5 mM $\text{C}_6\text{H}_5\text{Na}_3\text{O}_7 \cdot 2\text{H}_2\text{O}$, 11 mM NaH_2PO_4 , 10 mM MgSO_4 , 30 g/L NZ BL4 soy peptone (Kerry Bioscience, #5X00043), 15 g/L yeast extract (Teknova, #Y9020), 0.25 mL/L polypropylene glycol 2000, trace elements, and 10 mg/mL tetracycline. Salt feeds containing 75 mM $(\text{NH}_4)_2\text{SO}_4$, 150 mM K_2HPO_4 , 110 mM KH_2PO_4 , 7 mM $\text{C}_6\text{H}_5\text{Na}_3\text{O}_7 \cdot 2\text{H}_2\text{O}$, and 100 mM NaH_2PO_4 were started after 6 h at 25 g/h and continued for 8 h. Cultures were grown at 37 °C for 17 h before shifting the temperature to 26 °C and adding 27 mL of 1 M MgSO_4 . The carbon source consisted of a 70% glycerol feed, with roughly 2 L being fed over the course of the run. After 48 h, the cultures were harvested by centrifugation, yielding cell pellets of approximately 1 kg by wet weight. The pellets were stored at -80 °C until purification was commenced.

Purification of XTEN-1, 2, 3, 4. The cell pellet from each of the thiol-containing XTEN precursors (XTEN-1, 2, 3, 4) was resuspended in lysis buffer (20 mM Na-phosphate, pH 8.0, 5 mM imidazole, 500 mM NaCl) at a ratio of 3 mL buffer per gram of pellet and lysed using a dynamic high pressure homogenizer. The resulting cell lysates were heat-treated at 85 °C for 20 min, rapidly cooled to <10 °C in an ice bath, then clarified by centrifugation in a Sorvall RC-SB centrifuge at 10 000 rpm for 60 min. The supernatants were passed through a 0.22 μm filter.

Capture immobilized metal ion affinity chromatography (IMAC) was performed using Toyopearl AF-Chelate-650 M (Tosoh Bioscience) flow-packed columns. For each protein, columns were charged with NiSO_4 and equilibrated with 20 mM sodium phosphate, pH 8.0, 500 mM NaCl, and 5 mM imidazole prior to loading the clarified lysate. The columns were then washed with 20 mM sodium phosphate, pH 8.0, and 5 mM imidazole before being eluted with 20 mM sodium phosphate, pH 8.0, and 100 mM imidazole.

Fractions were evaluated for eluted protein by SDS-PAGE analysis and Coomassie staining, pooled, and digested overnight at 37 °C using bovine trypsin (Sigma) for removal of the purification and expression tags. The digests were verified using MALDI-TOF MS the next day before the addition of 2 mM EDTA and 20 mM DTT and heating to 85 °C to inactivate any residual trypsin and convert all cysteines to their reduced form.

Next, a polishing anion exchange chromatography (AEX) step was performed using columns packed with MacroCap Q (GE Healthcare Life Sciences) resin and equilibrated with 20 mM HEPES, pH 7.0. The trypsin digests were filtered prior to loading onto the columns, which were subsequently chased with equilibration buffer. Protein was eluted over gradient from 0 to 250 mM NaCl, 20 mM HEPES, pH 7.0, and elution fractions were pooled based on SDS-PAGE analysis and silver staining.

As a final step, the pooled proteins were concentrated and buffer exchanged into the formulation buffer (20 mM HEPES pH 7.0, 50 mM NaCl) using Biomax-5 Pellicon XL ultrafiltration cassettes (Millipore). XTEN protein concentrations were determined by amino acid analysis (AAA Service

Laboratory, Damascus, OR, USA) and quality was assessed by SDS-PAGE analysis with silver staining, analytical C4 reverse phase chromatography (RPC), analytical size-exclusion chromatography (SEC), and electrospray ionization mass spectrometry (ESI-MS).

Preparation of T-20-XTEN Conjugates. Lyophilized MPA-T-20 free acid was freshly dissolved in anhydrous DMF to a final concentration of 25 mM for the synthesis of the T-20-XTEN conjugates (T-20-XTEN-1, 2, 3, 4). Pilot-scale experiments were carried out first to optimize the reaction conditions. MPA-T-20 was reacted with 1 \times Thiol-XTEN (XTEN-1) at a molar ratio of 2:1 (MPA-T-20:XTEN) for 2 h at 25 °C, with the reaction mixture analyzed by C4 RPC to determine the extent of conversion. 3 \times Thiol-XTENs were diluted 2-fold into DMF to facilitate the solubility of MPA-T-20 in the reaction mixtures, and MPA-T-20 was added at molar ratios of 3:1, 6:1, and 12:1 (MPA-T-20:XTEN) for 4 h at 25 °C, with the reaction mixtures monitored by C4 RPC at 1, 2, and 4 h to track the extent of conversion.

For the large scale syntheses, 100 mg of 1 \times Thiol-XTEN (XTEN-1) was diluted 2-fold into DMF to facilitate peptide solubility and reacted with MPA-T-20 (MPA-T-20:XTEN = 2:1) for 2 h at 25 °C. The reaction mixture was analyzed by C4 RPC to determine the extent of conversion to the 1 \times T-20-XTEN conjugate (T-20-XTEN-1). Approximately 100 mg of 3 \times Thiol-XTENs (XTEN-2, 3, 4) were similarly diluted 2-fold into DMF and reacted with MPA-T-20 (MPA-T-20:XTEN = 3:1) for 4 h at 25 °C. The reaction mixtures were analyzed by C4 RPC to determine the extent of conversion to the 3 \times T-20-XTEN (T-20-XTEN-2, 3, 4) conjugates. The negative control (XTEN-1A) was prepared by reacting 1 \times Thiol XTEN (XTEN-1) with free 3-maleimidopropionic acid in a 2:1 ratio (MPA:XTEN) for 2 h at 25 °C; the end products were also confirmed and analyzed by C4 RPC.

Preparative C4 RPC of T-20-XTEN Conjugates. The T-20-XTEN conjugates (T-20-XTEN-1, 2, 3, 4) and the negative control (XTEN-1A) were purified by preparative C4 RPC using a Vydac 214TP C4 10 μm 300 Å 22 \times 250 mm column (Grace Davison Discovery Sciences). Buffer A was 0.1% TFA in water, and buffer B was 0.1% TFA in 100% acetonitrile. The system and column were equilibrated in a solution of 5% buffer B and 95% buffer A at a flow rate of 10 mL/min at ambient temperature. Separation was achieved with a gradient from 5% to 50% buffer B over 70 min at a flow rate of 10 mL/min. Fractions containing the fully modified T-20-XTEN conjugates were neutralized, concentrated by vacuum centrifugal evaporation, and then buffer exchanged into PBS buffer (Life Technologies, Carlsbad, CA) using 5 kDa molecular weight cutoff (MWCO) Vivaspin 15 mL centrifugal filters (Sartorius Stedim Biotech) for storage at -80 °C. T-20-XTEN conjugate concentrations were assayed by measuring their absorbances at 280 nm, and quality was assessed by analytical C4 RPC, analytical SEC, ESI-MS, and dynamic light scattering (DLS).

SDS-PAGE Analysis. SDS-PAGE was performed using NuPAGE Bis-Tris 4–12% gradient gels, NuPAGE MOPS SDS running buffer, and Novex Sharp Standard (Life Technologies). The thiol-containing XTEN precursors (XTEN-1, 2, 3, 4) were reduced with 10 mM DTT prior to analysis. The XTEN peptide conjugates were loaded directly on the gels without reduction. Separation was performed for 40 min at 200 V, and the gels were stained using SimplyBlue SafeStain (Life Technologies) or a Pierce Silver Stain Kit (Thermo Scientific).

Analytical Size-Exclusion Chromatography. Analytical SEC was performed using a BioSep-SEC-s4000 7.8 × 600 mm HPLC column (Phenomenex) connected to an LC2010 integrated HPLC system (Shimadzu). The system and column were equilibrated using 50 mM sodium phosphate, pH 6.5, and 300 mM NaCl at a flow rate of 0.5 mL/min at ambient temperature. For column calibration, a SEC column standard (Phenomenex) was used. To analyze the samples, 20 μ g of protein was injected in a 3 to 5 μ L volume and eluted from the column at a flow rate of 0.5 mL/min. The absorbance was monitored at 214 nm for 70 min to track the progress of the protein sample.

Analytical C4 Reverse Phase Chromatography. Analytical C4 RPC was performed using a Vydac 214TP C4 5 μ m 300 Å 4.6 × 150 mm column (Grace Davison Discovery Sciences) connected to an LC2010 integrated HPLC system (Shimadzu). Buffer A was 0.1% trifluoroacetic acid (TFA) in water and buffer B was 0.1% TFA in 100% acetonitrile. The system and column were equilibrated in a solution of 5% buffer B and 95% buffer A at a flow rate of 1 mL/min at ambient temperature. For sample analysis, 20 μ g of protein was injected in a 20 μ L volume. Separation was achieved using a linear gradient from 5% to 50% B over 45 min at a flow rate of 1 mL/min, and the absorbance was monitored at 214 nm to track the progress of the protein sample.

Electrospray Ionization Mass Spectrometry. 100 μ g of purified protein was desalted by buffer exchange against 0.5% formic acid in water using 5 kDa MWCO Vivaspin 500 μ L centrifugal filters (Sartorius Stedim Biotech). The retentate was recovered in a 100 μ L volume, mixed with an equal volume of acetonitrile, and infused at a flow rate of 10 μ L/min into a QSTAR XL mass spectrometer (AB Sciex). Multicharge time-of-flight spectra were acquired in the 800 to 1600 amu range. Zero-charge spectra were obtained by Bayesian reconstruction in the 10 to 100 kDa range.

Dynamic Light Scattering. The T-20-XTEN conjugates (T-20-XTEN-1, 2, 3, 4), the negative control (XTEN-1A), and a positive control (BSA, Fermentas) were centrifuged for 15 min at 18 000 g and transferred to clean, disposable cuvettes (Eppendorf) for analysis in a DynaPro Titan dynamic light scattering instrument (Wyatt Technologies). Readings were taken at 100% laser power until consistent intensity readings were obtained, and 15 measurements were collected for each sample to generate the particle size distribution using a regularization fit. Both the effective radius and the aggregations by intensity and mass were reported for each sample. The positive control was heat treated at 80 °C for 10 min and cooled on ice for 5 min before being analyzed a second time.

Antiviral MAGI Assay. A multinuclear activation of a galactosidase indicator (MAGI) assay was performed at Southern Research Institute (Frederick, MD) with MAGI CCR5 cells to test the activity of the T-20-XTEN conjugates. MAGI CCR5 cells originate from a HeLa cell line that constitutively expresses CXCR4 and is engineered to express high levels of CD4 and CCR5, as well as contain one copy of the HIV-1 LTR promoter driving the expression of the β -galactosidase gene upon HIV-1 Tat transactivation.²⁷ On the day preceding the assay, 1 × 10⁴ cells per well were plated and allowed to adhere overnight at 37 °C. The media used for plating the cells was aspirated and exchanged with a range of concentrations (up to 10 nM) of the T-20-XTEN conjugates (T-20-XTEN-1, 2, 3, 4), followed by the introduction of the HIV-1_{Ba-L} virus. The cultures were then incubated for 48 h, after

which the cells were lysed and β -galactosidase enzyme activity measured upon the addition of Gal-screen reagent (Tropix, Bedford, MA). The T-20 peptide without MPA (Southern Research Institute, Frederick, MD) and XTEN-1A were respectively used as the positive and negative controls, and all samples were tested in triplicate. As a measure of compound toxicity, parallel cytotoxicity plates were set up for which the virus was replaced with media and the cytotoxicity was monitored by MTS staining (Promega, Madison, WI). The IC₅₀ for inhibition of virus replication and the TC₅₀ for cytotoxicity of the tested compounds were determined based on this analysis.

Rat Pharmacokinetics. T-20-XTEN-4, the compound with the strongest antiviral activity, was administered by subcutaneous injection at 1.92 mg/kg into three female Sprague-Dawley rats. Blood samples were collected in prechilled heparinized tubes predose as well as at 1, 3, 8, 12, 24, 48, 72, 96, and 120 h post-administration. The samples were processed to heparin plasma and stored immediately at −80 °C. Plasma samples were analyzed using a sandwich anti-XTEN/anti-XTEN enzyme-linked immunosorbent assay (ELISA) in 3% rat plasma, with purified T-20-XTEN-4 conjugate utilized as the calibration standard. The ELISA utilized a proprietary anti-XTEN mouse monoclonal antibody for capture, a biotinylated anti-XTEN antibody for detection, and streptavidin-horse-radish peroxidase (Pierce #21130) with 3,3',5,5'-tetramethylbenzidine peroxidase substrate (Immunochemistry Technologies, SUBI) for development.⁶ Following absorbance readings at 450 nm, protein concentrations were determined using a standard curve fitted using a 4 parameter model and back-calculated to their values in 100% plasma. Pharmacokinetic curves were averaged for the three assayed rats, with analyses performed using PK Solutions 2.0 software (Summit Research Services, Montrose, CO, USA).

■ ASSOCIATED CONTENT

● Supporting Information

Supplementary figure describing the RP-HPLC profiles of the XTEN precursors. This material is available free of charge via the Internet at <http://pubs.acs.org>.

■ AUTHOR INFORMATION

Corresponding Author

*E-mail: vschellenberger@amunix.com.

Notes

The authors declare no competing financial interest.

■ ACKNOWLEDGMENTS

This work was supported by the NIH Small Business Innovation Research (SBIR) grant program (Grant Number: 1R43AI102765-01).

■ ABBREVIATIONS

AAA, amino acid analysis; AEX, anion exchange chromatography; DLS, dynamic light scattering; IMAC, immobilized metal affinity chromatography; MAGI, multinuclear activation of a galactosidase indicator; MPA, 3-maleimidopropionamide; PEG, poly(ethylene glycol); RP-HPLC, reverse-phase high pressure liquid chromatography; RPC, reverse phase chromatography; SDS-PAGE, sodium dodecyl sulfate polyacrylamide gel electrophoresis; SEC, size-exclusion chromatography

■ REFERENCES

- (1) Kontermann, R. E. (2011) Strategies for extended serum half-life of protein therapeutics. *Curr. Opin. Biotechnol.* 22, 868–76.
- (2) Jevsevar, S., Kusterle, M., and Kenig, M. (2012) PEGylation of antibody fragments for half-life extension. *Methods Mol. Biol.* 901, 233–46.
- (3) Veronese, F. M., and Pasut, G. (2005) PEGylation, successful approach to drug delivery. *Drug Discovery Today* 10, 1451–8.
- (4) Yang, Z., Wang, J., Lu, Q., Xu, J., Kobayashi, Y., Takakura, T., Takimoto, A., Yoshioka, T., Lian, C., Chen, C., Zhang, D., Zhang, Y., Li, S., Sun, X., Tan, Y., Yagi, S., Frenkel, E. P., and Hoffman, R. M. (2004) PEGylation confers greatly extended half-life and attenuated immunogenicity to recombinant methioninase in primates. *Cancer Res.* 64, 6673–8.
- (5) Schellenberger, V., Wang, C. W., Geething, N. C., Spink, B. J., Campbell, A., To, W., Scholle, M. D., Yin, Y., Yao, Y., Bogin, O., Cleland, J. L., Silverman, J., and Stemmer, W. P. (2009) A recombinant polypeptide extends the in vivo half-life of peptides and proteins in a tunable manner. *Nat. Biotechnol.* 27, 1186–90.
- (6) Alters, S. E., McLaughlin, B., Spink, B., Lachinyan, T., Wang, C. W., Podust, V., Schellenberger, V., and Stemmer, W. P. (2012) GLP2–2G-XTEN: a pharmaceutical protein with improved serum half-life and efficacy in a rat Crohn's disease model. *PLoS One* 7, e50630.
- (7) Cleland, J. L., Geething, N. C., Moore, J. A., Rogers, B. C., Spink, B. J., Wang, C. W., Alters, S. E., Stemmer, W. P., and Schellenberger, V. (2012) A novel long-acting human growth hormone fusion protein (VRS-317): enhanced in vivo potency and half-life. *J. Pharm. Sci.* 101, 2744–54.
- (8) Geething, N. C., To, W., Spink, B. J., Scholle, M. D., Wang, C. W., Yin, Y., Yao, Y., Schellenberger, V., Cleland, J. L., Stemmer, W. P., and Silverman, J. (2010) Gcg-XTEN: an improved glucagon capable of preventing hypoglycemia without increasing baseline blood glucose. *PLoS One* 5, e10175.
- (9) Yuen, K. C., Conway, G. S., Popovic, V., Merriam, G. R., Bailey, T., Hamrahian, A. H., Biller, B. M., Kipnes, M., Moore, J. A., Humphriss, E., Bright, G. M., and Cleland, J. L. (2013) A long-acting human growth hormone with delayed clearance (VRS-317): results of a double-blind, placebo-controlled, single ascending dose study in growth hormone-deficient adults. *J. Clin. Endocrinol. Metab.* 98, 2595–603.
- (10) Gaberc-Porekar, V., Zore, I., Podobnik, B., and Menart, V. (2008) Obstacles and pitfalls in the PEGylation of therapeutic proteins. *Curr. Opin. Drug Discovery Dev.* 11, 242–50.
- (11) Podust, V. N., Sim, B. C., Kothari, D., Henthorn, L., Gu, C., Wang, C. W., McLaughlin, B., and Schellenberger, V. (2013) Extension of in vivo half-life of biologically active peptides via chemical conjugation to XTEN protein polymer. *Protein Eng. Des. Sel.* 26, 743–53.
- (12) Matthews, T., Salgo, M., Greenberg, M., Chung, J., DeMasi, R., and Bolognesi, D. (2004) Enfuvirtide: the first therapy to inhibit the entry of HIV-1 into host CD4 lymphocytes. *Nat. Rev. Drug Discovery* 3, 215–25.
- (13) Chan, D. C., and Kim, P. S. (1998) HIV entry and its inhibition. *Cell* 93, 681–4.
- (14) Naider, F., and Anglister, J. (2009) Peptides in the treatment of AIDS. *Curr. Opin. Struct. Biol.* 19, 473–82.
- (15) Lalezari, J. P., Henry, K., O'Hearn, M., Montaner, J. S., Piliero, P. J., Trottier, B., Walmsley, S., Cohen, C., Kuritzkes, D. R., Eron, J. J., Jr., Chung, J., DeMasi, R., Donatucci, L., Drobnes, C., Delehanty, J., and Salgo, M. (2003) Enfuvirtide, an HIV-1 fusion inhibitor, for drug-resistant HIV infection in North and South America. *N. Engl. J. Med.* 348, 2175–85.
- (16) Huet, T., Kerbarh, O., Schols, D., Clayette, P., Gauchet, C., Dubreucq, G., Vincent, L., Bompais, H., Mazinghien, R., Querolle, O., Salvador, A., Lemoine, J., Lucidi, B., Balzarini, J., and Petitou, M. (2010) Long-lasting enfuvirtide carrier pentasaccharide conjugates with potent anti-human immunodeficiency virus type 1 activity. *Antimicrob. Agents Chemother.* 54, 134–42.
- (17) Garay, R. P., El-Gewely, R., Armstrong, J. K., Garratty, G., and Richette, P. (2012) Antibodies against polyethylene glycol in healthy subjects and in patients treated with PEG-conjugated agents. *Exp. Opin. Drug Delivery* 9, 1319–23.
- (18) Chang, C. H., Hinkula, J., Loo, M., Falkeborn, T., Li, R., Cardillo, T. M., Rossi, E. A., Goldenberg, D. M., and Wahren, B. (2012) A novel class of anti-HIV agents with multiple copies of enfuvirtide enhances inhibition of viral replication and cellular transmission in vitro. *PLoS One* 7, e41235.
- (19) Welch, B. D., Francis, J. N., Redman, J. S., Paul, S., Weinstock, M. T., Reeves, J. D., Lie, Y. S., Whitby, F. G., Eckert, D. M., Hill, C. P., Root, M. J., and Kay, M. S. (2010) Design of a potent D-peptide HIV-1 entry inhibitor with a strong barrier to resistance. *J. Virol.* 84, 11235–44.
- (20) Francis, J. N., Redman, J. S., Eckert, D. M., and Kay, M. S. (2012) Design of a modular tetrameric scaffold for the synthesis of membrane-localized D-peptide inhibitors of HIV-1 entry. *Bioconjugate Chem.* 23, 1252–8.
- (21) Silverman, J., Liu, Q., Bakker, A., To, W., Duguay, A., Alba, B. M., Smith, R., Rivas, A., Li, P., Le, H., Whitehorn, E., Moore, K. W., Swimmer, C., Perlroth, V., Vogt, M., Kolkman, J., and Stemmer, W. P. (2005) Multivalent avimer proteins evolved by exon shuffling of a family of human receptor domains. *Nat. Biotechnol.* 23, 1556–61.
- (22) Clavel, F., and Hance, A. J. (2004) HIV drug resistance. *N. Engl. J. Med.* 350, 1023–35.
- (23) Este, J. A., and Telenti, A. (2007) HIV entry inhibitors. *Lancet* 370, 81–8.
- (24) Eggink, D., Baldwin, C. E., Deng, Y., Langedijk, J. P., Lu, M., Sanders, R. W., and Berkhout, B. (2008) Selection of T1249-resistant human immunodeficiency virus type 1 variants. *J. Virol.* 82, 6678–88.
- (25) He, Y., Xiao, Y., Song, H., Liang, Q., Ju, D., Chen, X., Lu, H., Jing, W., Jiang, S., and Zhang, L. (2008) Design and evaluation of sifuvirtide, a novel HIV-1 fusion inhibitor. *J. Biol. Chem.* 283, 11126–34.
- (26) Ray, N., Harrison, J. E., Blackburn, L. A., Martin, J. N., Deeks, S. G., and Doms, R. W. (2007) Clinical resistance to enfuvirtide does not affect susceptibility of human immunodeficiency virus type 1 to other classes of entry inhibitors. *J. Virol.* 81, 3240–50.
- (27) Kimpton, J., and Emerman, M. (1992) Detection of replication-competent and pseudotyped human immunodeficiency virus with a sensitive cell line on the basis of activation of an integrated beta-galactosidase gene. *J. Virol.* 66, 2232–9.